Effects of elevated sulfate in eutrophic waters on the internal phosphate release under oxic conditions across the sediment-water interface

Jun Chen[1, 2], Honggang Zhang[1, 5], Lixuan Liu[6], Jing Zhang[1], Mick Cooper[3, 4], Robert J. G. Mortimer [7, 8], Gang Pan[1, 3, 4, 8*]

[1]*Research Center for Eco-Environmental Sciences, Chinese Academy of Sciences, Beijing 100085, China*

[2]*University of Chinese Academy of Sciences, Beijing, 100049, China*

[3]*School of Animal, Rural and Environmental Sciences, Nottingham Trent University, Brackenhurst Campus, NG25 0QF, UK*

[4]*Integrated Water-Energy-Food Facility (iWEF), Nottingham Trent University, Nottinghamshire NG25 0QF, UK*

[5]*Yangtze River Delta Branch, Research Center for Eco-Environmental Sciences, Chinese Academy of Sciences, Yiwu 322000, China*

[6]*High-Tech Research Institute Beijing University of Chemical Technology Beijing, China*

[7] *York St John University, Lord Mayor's Walk, York YO31 7EX, UK*

[8] Nanjing Xianglai Institute of Eco-environmental Science and Technology, Nanjing 210046, China

* Corresponding authors: gang.pan@ntu.ac.uk (Gang Pan)

Abstract

Eutrophication in freshwater environments may be enhanced by the elevation of sulfate in waters, through the release of internal phosphorus (P) from anoxic sediments. However, the influence of increasing but modest sulfate concentrations (less than 3,000 μM) on P release under oxic conditions across the sediment-water interface (SWI) in eutrophic freshwater is poorly understood. In this study, the profiles of P, iron (Fe), ~~and~~ sulfur (S) and physicochemical parameters were measured in a simulated lacustrine system with varying concentrations of sulfate (970-2,600 μM) in overlying water. The results indicated that elevated concentrations of sulfate increased the soluble reactive P in overlying waters under oxic conditions across the SWI. A 100 μM increase of sulfate was found to induce a 0.128 mgm^{-2}d^{-1} increase of P flux from surface sediments into overlying waters under oxic conditions. Higher sulfate concentrations in the overlying waters increased the concentrations of labile S(-II) in the deep sediments, due to sulfate penetration and subsequent reduction to S(-II). We also found the fluxes of labile Fe and P from deep to surface sediment were both positive and greater than the corresponding fluxes from surface sediment to the overlying water, suggesting that reduction of P-bearing Fe(III)(oxyhydr)oxides in deep anoxic sediment acted as a major source of internal P release. In addition, the upward flux of Fe(II) was significantly lower under higher sulfate conditions, indicating that the Fe(II) flux could be blocked ~~mitigated~~ by formation of Fe(II) sulfides in the deep sediment. Under these conditions, less Fe(II) from deep sediments could be re-oxidized and combine with P in the surface,

39   oxic sediment, thereby reducing the retention capacity for P and leading to higher

40   release of internal P to the water column.

41   **Key words:** Eutrophication, Internal P loading, Sulfate, Freshwater, DGT

42   **1. Introduction**

43   Eutrophication and the consequent formation of harmful algal blooms (HABs)

44   represents a global challenge and poses serious threats to ecosystem services and human

45   health (Conley et al. 2009, Paerl et al. 2011, Smith 2003). Phosphorus (P) is regarded

46   as one of the primary limiting factors for the control of eutrophication in freshwater

47   (Carpenter 2008, Schindler et al. 2008). Measures aimed at reducing inputs of external

48   phosphorus have resulted in large-scale declines of phosphorus concentrations in many

49   water bodies around the world (Huser et al. 2018, Tong et al. 2017). However, lakes

50   typically show a delayed recovery in response to decreasing external P loads (Coveney

51   et al. 2005), due to release of internal P from sediments (Paytan et al. 2017). Thus,

52   understanding the processes of P release from sediments is important for the successful

53   management of eutrophic waters.

54   The process of internal P release is influenced by many factors, such as

55   temperature, pH and redox conditions (Christophoridis and Fytianos 2006). Iron (Fe) is

56   a redox-sensitive element and the biogeochemical cycling of Fe regulates the mobility

57   of internal phosphorus (Mortimer 1942). Under anoxic conditions, the reductive

58   dissolution of P-bearing Fe(III)(oxyhydr)oxides is recognized as a major mechanism

59   for internal P release (Rydin 2000). However, comparison of 23 different aquatic

60 systems did not show a strong correlation between internal P release rate and the bottom

61 water oxygen concentration (Caraco et al. 1989). In addition, the sulfate concentration

62 of the water was regarded as an extremely important variable controlling sediment P

63 release in multiple systems, and showed a strong correlation with P release rate under

64 both oxic and anoxic conditions (Caraco et al. 1989). Thus, the amount of P released

65 from the sediment depended on the availability of sulfate (Caraco et al. 1989).

66   It has been found that the sulfide produced during sulfate reduction promote P

67 mobilization from marine sediment through its dual effect on the cycling of Fe

68 (Lehtoranta et al. 2009, Roden and Edmonds 1997, Rozan et al. 2002). Firstly, sulfide

69 is a powerful reductant for the reduction of solid Fe(III) minerals to dissolved Fe(II)

70 ion with concurrent P release (Bostrom et al. 1988). Secondly, sulfide could displace P

71 from solid-phase Fe(II)-P compounds and trap the dissolved Fe(II) ion to iron sulfide

72 precipitation (Roden and Edmonds 1997), which significantly promotes P release and

73 reduces P retention capacity (Lehtoranta et al. 2009). For freshwater lakes with low

74 concentrations of sulfate, it is commonly accepted that sulfate has slight effect on

75 internal P release and Fe cycling (Caraco et al. 1989, Hansel et al. 2015). During recent

76 decades, sulfate concentrations have increased in freshwater systems due to acid

77 deposition and industrial wastewater inputs (Yu et al. 2013, Zak et al. 2006). For

78 example, sulfate concentration in Lake Taihu has undergone a rapid increase (>12 μM

79 $L^{-1}y^{-1}$) over the past 60 years and now attains concentrations close to 1,000 μM (Yu et

80 al. 2013). Caraco et al. (1989) proposed that freshwater systems with intermediate

81   sulfate concentration (~100-300 μM sulfate) tended to have high P release rates under

82   anoxic condition. Some researchers showed that increasing sulfate levels could

83   significantly promote the internal P release in freshwater lakes under anoxic conditions

84   (Chen et al. 2016a, Roden and Edmonds 1997, Zhao et al. 2019). So far, anoxic

85   conditions in the bottom water could be considered as an essential prerequisite for

86   sulfate-stimulated release of P from sediments in freshwater systems.

87   Under natural conditions, oxygen distribution across the sediment-water interface

88   (SWI) in shallow freshwater lakes, like Lake Taihu in China, is heavily influenced by

89   hydrodynamic disturbance, accelerating the oxygen diffusion rate from the atmosphere

90   to the water column (Chatelain and Guizien 2010). Thus, anoxia in bottom waters is

91   hardly persistent during most seasons, except in the summer months. In the oxygenated

92   water column and oxic surface sediments, Fe(II) may be rapidly converted to

93   Fe(III)(oxyhydr)oxides, which provide fresh adsorption sites on which to retain

94   available P (Mortimer 1942). Although oxic conditions across the SWI may increase

95   the P adsorption capacity in surface sediment, P release is still observed in some oxic

96   bottom waters (Gächter and Müller 2003, Kraal et al. 2013). These observations suggest

97   that other mechanisms may also affect internal P release. For example, P can be released

98   by dissolution of vivianite by interaction with hydrogen sulfide in deep sediments

99   where oxygen cannot diffuse (Gächter and Müller 2003). Thus, higher concentrations

100   of hydrogen sulfide in deep sediments may influence P release from surface sediments

101   under oxic SWI conditions. Hansel et al. (2015) found that even when the sulfate

102 concentration was as low as 200 μM, sulfate reduction was still a dominate force for

103 the reduction of Fe(III) oxide. Increasing concentration of the sulfate in freshwater lakes

104 has the potential to promote the mobilization of P through its effect on the cycling of

105 iron under oxic condition across the SWI. However, to date no quantitative analysis has

106 been undertaken on the contribution of elevated sulfate in shallow freshwaters to

107 internal P release under oxic SWI conditions. Work to date has only been undertaken

108 on sulfate rich waters such as a lowland river (2,600-7,800 μM sulfate) polluted by

109 mining activities and an estuary (28,000 μM sulfate) (Kraal et al. 2013, Zak et al. 2006),

110 neither of which has wide applicability for freshwater systems. In addition, a

111 comprehensive evaluation of the impact of sulfate on the dynamic cycling of S-Fe-P,

112 and their interactions, is crucial to the understanding of how eutrophication conditions

113 change with oxic-anoxic variations.

114 In this study, an incubation experiment was conducted in a continuous dynamic

115 shallow water simulation system under three sulfate levels. Diffusive gradients in thin

116 films (DGT) and microelectrode techniques were employed to collect the vertical

117 dynamic features of labile of P, Fe, S, as well as the related environmental factors at a

118 fine scale. Based on the DGT profiles, the apparent fluxes of labile P and Fe from both

119 surface sediment to water, and from deep sediment to surface sediment, were calculated.

120 The objective of the study was to explore the effects of elevated sulfate inputs to the

121 water column under oxic SWI conditions on internal P release.

2. Materials and methods

2.1. Sample Collection

The sampling sites were in Meiliang Bay (120°9 E, 31°31 N), the northern part of Lake Taihu. Lake Taihu is the third largest freshwater lake in China and is experiencing eutrophication and algal blooms. Sulfate concentrations here have undergone a rapid increase over the past 60 years and now attain about 1,000 μM (Yu et al. 2013). Sediments and lake water were collected from Lake Taihu using an Ekman grab sampler and Plexiglas hydrophore, respectively. The collected samples were transported to the laboratory immediately and stored at 4 °C for less than 24 h before pre-treatment.

2.2. Preparation of sediment-water columns

Sediments were sieved through a 0.5 mm pore-size mesh to remove occasional macrofauna and large particles, and then completely homogenized to eliminate the horizontal heterogeneity of the natural sediment (Ding et al. 2015, Zilius et al. 2016). The pre-treated sediments and overlying water (filtered with 0.45 μm filters) were used to fill perspex cylinders (8.4 cm in diameter and 50 cm in height) and 48 cylinders were produced in this study. Each cylinder contained 20 cm of sediment and 25 cm of overlying water. This sediment pretreatment method has been used extensively in other incubation experiments focused on exchange across the SWI (Chen et al. 2016b, Sun et al. 2017, Wang et al. 2017).

2.3. Microcosm set-up

Water flow over sediment has a significant influence on oxygen consumption

7

143   (Higashino 2011) and water-sediment interaction (Qin et al. 2007), which play key roles

144   in Fe-S-P cycling. Taking this into consideration, we designed a dynamic microcosm

145   system. The microcosm system consisted of six units, each including a water reservoir

146   tank (12.3 cm in diameter and 20 cm in height) and six perspex cylinders (Figure.S1a

147   and b). All of the cylinders were sealed with rubber plugs and silicone sealant. A micro

148   pump and an aeration unit were installed in each reservoir tank (Figure.S1c). Water

149   from each of the reservoir tanks was separately pumped into the inlet of the first

150   cylinder of each unit, at 5 cm above the surface of sediment, and flowed out through

151   the outlet of the cylinder, into the inlet of the next cylinder in the unit. All six cylinders

152   in one unit were connected in series via their inlets and outlets, to simulate the regular

153   water movement in shallow lakes and uniform initial conditions among cylinders. The

154   water in the final cylinder of a unit flowed into the reservoir tank of the next unit. Water

155   in each reservoir tank was initially sparged with N_2 at a flow rate of 0.4 L min^{-1} for 24

156   h to remove oxygen from each unit and then air was pumped into each tank for 5 min

157   h^{-1} to maintain the oxic environment across the SWI. The pre-incubation period lasted

158   for 2 weeks.

159   At the end of pre-incubation, the concentrations of dissolved oxygen (DO), redox

160   potential (Eh), DGT-labile P and Fe, and the soluble reactive P (SRP) in water-sediment

161   profiles were measured from three randomly selected cylinders (Figure.S2). The

162   profiles exhibited very consistent distributions for all the parameters, suggesting that

163   the sediment was homogeneous in chemical distribution across different cylinders prior

164 to the main experiments.

165 *2.4. Incubation Experiment*

166   After pretreatment, the water in each of the final cylinders in a unit was directed

167 back to that unit's own reservoir tank, and the entire microcosm was separated into

168 eight independent units (Figure.S1b). We choose six units (36 cylinders) at random on

169 which to perform the experiment. $Na_2SO_{4(S)}$ was subsequently dissolved in the

170 corresponding reservoir tank to obtain the desired concentration values as follows: no

171 addition (Control; group C), 1,770 μM (low sulfate; group B), and 2,600 μM (high

172 sulfate; group A). Control group (970 μM) represented the background concentration

173 of sulfate found in the water column of Lake Taihu. According the work of Caraco et

174 al. (1989), the background concentration of sulfate (~1000 μM) in Lake Taihu is higher

175 than the typical freshwater type (~10-300 μM). However, it is still much less sulfate

176 rich than the sites (a lowland river (2,600-7,800 μM sulfate) polluted by mining

177 activities and an estuary (28,000 μM sulfate)) studied previously (Kraal et al. 2013, Zak

178 et al. 2006). As no mandatory standards of sulfate are declared for surface waters

179 worldwide, we chose the quality standard of sulfate in drinking water (2,600 μM) in

180 China (GB3838-2002, China) for the high sulfate group (group A), which was very

181 close to lower limiting values of salt waters (~3,000-30,000 μM). The set value in group

182 B was a median value between those for groups A and C. All three units were incubated

183 at room temperature (20±2 °C) for 45 days in the dark. Sampling was performed on the

184 10th, 20th, 30th, 32nd, 37th and 45th day after the onset of incubation.

2.5. Analyses of samples

186   On the planned sampling day, two columns for each treatment (treated as duplicates)

187   were randomly selected for sediment and water sampling. The distribution of DO and

188   Eh in water-sediment profiles were measured using needle-type microelectrodes (OX-

189   100 and RD-100; Unisense, Denmark) and the overlying water was then collected.

190   Subsequently, ZrO-Chelex and AgI DGT (Easysensor Ltd., China) probes bound back

191   to back were inserted into the sediments (Han et al. 2015). 24 hours later, these DGT

192   probes were retrieved from sediments for processing.

193   After that, the sediment samples were transferred to a glove box containing a dry

194   nitrogen atmosphere and sliced at a vertical resolution of 1cm to a depth of 10cm. An

195   aliquot of each sliced sediment sample was transferred to a 50 ml plastic centrifuge tube

196   which was then capped, removed from the glove box and centrifuged at 2500 g for 30

197   min. After centrifugation, tubes were returned to the glove box to sample the pore water.

198   The supernatant water in each centrifuge tube was dispensed via a 10 ml plastic syringe,

199   fitted with a 0.45μm pore-size cellulose nitrate membrane filter, collected in a 5 ml

200   plastic centrifuge tube, and finally stored at -20 °C. (Modified from Jilbert et al. (2011)).

201   The deployed ZrO-Chelex DGT was analyzed following the procedure detailed in

202   Xu et al. (2013). The ZrO-Chelex gel was sliced at a resolution of 2 mm. Each sliced

203   gel was sequentially eluted using HNO_3 and NaOH and the labile P and Fe in the eluates

204   were determined using a microplate spectrophotometer (Multiskan FC; Thermo

205   Scientific, Waltham, USA). The concentrations of labile S contained in the binding

206   layer of the AgI DGT were determined by computer imaging densitometry (CID). The

207 image of the AgI gel was scanned using a flat-bed scanner (Canon 5600F, Canon Inc.,

208 Japan) at a resolution of 600 dpi (0.0423 mm×0.0423 mm) and then converted to

209 grayscale intensities with Image J (Version 1.48, NIH, USA) (Ding et al. 2012). The

210 concentrations of the labile P, Fe and S measured by the DGT were calculated by

211 methods listed in the Supporting Information.

212 The concentration of SRP in the water was determined using the molybdenum blue

213 method (Murphy and Riley 1962). The concentration of sulfate in water was measured

214 using a turbid metric method (Tabatabai 1974).

215 *2.6. Data processing*

216 ~~To reflect the diffusion direction of Fe and P across the sediment-water interface~~

217 ~~and oxic-anoxic interface.~~ To assess the effect of elevated sulfate in overlying water on

218 internal P release under oxic condition across the SWI, the apparent fluxes at two depths

219 were calculated in this study. Oxygen penetration depths in the sediment were measured

220 as being less than 1cm (Fig.2.b). Therefore, this depth (-1 cm) was used to divide

221 sediment profiles into surface oxic sediment and deeper anoxic sediment.

222 The ~~net~~ apparent fluxes of P and Fe at a specific depth were calculated from the

223 DGT-labile P and labile Fe profiles using the following procedure:

224 (i) $C = f(x)$:get the regression equation between the measured concentrations (C) of

225 P or Fe(II) and the corresponding depth (x).

226 So, the concentration gradients at the depth of i: $\left.\dfrac{\partial c}{\partial x}\right|_{x=i} = f'(i)$ and the mean

227 concentration gradients from depth of m to depth of n: $\left.\dfrac{\overline{\partial c}}{\partial x}\right|_{mn} = \dfrac{\sum\limits_{i=m}^{n} f'(i)}{m-n}$. Based on the

228 depth-distributions of DGT-labile P and Fe, the concentration gradients were assessed

229   separately at the depths from 0 to1 cm (overlying water),0 to -1 cm (surface oxic

230   sediment), -1 to -10 cm (deep anoxic sediment)

231   (ii) Taking the main mechanisms that could influence the internal P release into

232   consideration, the ~~net~~ apparent fluxes of P or Fe(II) at the SWI were calculated as the

233   sum of fluxes from surface sediment to the SWI, and from bottom water to the SWI

234   using equation (1) (Ding et al. 2015, Gao et al. 2016).

235 $$F_0 = F_S + F_W = (-\varphi D_S \frac{\partial c_s}{\partial x_s}) + (-D_w \frac{\partial c_w}{\partial x_w}) \qquad (1)$$

236   Where F_0 is the apparent flux (mg m^{-2}d^{-1}) at the SWI. F_s and F_w represent the labile

237   P or Fe fluxes from surface sediment to the SWI, and form bottom water to the SWI,

238   respectively. $\frac{\partial c_s}{\partial x_s}$ and $\frac{\partial c_w}{\partial x_w}$ are the concentration gradients in surface sediment and

239   overlying water, respectively. φ is the porosity in sediment. D_w is the diffusion

240   coefficient in water (cm^2 s^{-1}) calibrated by the actual temperature (Li and Gregory 1974).

241   The diffusion coefficient in sediment (D_s) (cm^2 s^{-1}) were calculated from the diffusion

242   coefficient in water (D_w) and porosity (φ) in sediment (Ullman and Aller 1982). ~~Ds is~~

243   ~~the bulk sedimentary diffusion coefficient (cm² s⁻¹) (Ullman and Aller 1982). Dw is the~~

244   ~~bulk sedimentary diffusion coefficient in water, and the porosity is φ (Han et al. 2015,~~

245   ~~Li and Gregory 1974) ; $\frac{\partial c_s}{\partial x_s}$ and $\frac{\partial c_w}{\partial x_w}$ are the concentration gradients in surface~~

246   ~~sediment and overlying water, respectively.~~

247   (iii) Similarly, the ~~net~~ apparent fluxes of P or Fe(II) at 1 cm below the SWI (-1 cm)

248   were calculated using equation (2)

249 $$F_1 = F_{s1} + F_{s2} = (-\varphi D_{S1} \frac{\partial c_{s1}}{\partial x_{s1}}) + (-\varphi_2 D_{S2} \frac{\partial c_{s2}}{\partial x_{s2}}) \qquad (2)$$

250   Where ~~F₁ is the apparent flux at 1 cm below the SWI (-1 cm).~~ F_{s1} and F_{s2} represent

251   the labile P or Fe fluxes from surface sediment to -1 cm, and form deep sediment to -1

cm, respectively. F_1 is the and apparent flux at 1 cm below the SWI (-1 cm), which is the sum of F_{s1} and F_{s2} D_{s1}, φ_1, $\frac{\partial c_{s1}}{\partial x_{s1}}$, D_{s2}, φ_2, and $\frac{\partial c_{s2}}{\partial x_{s2}}$ were the mean values of sedimentary diffusion coefficients, porosity, and concentration gradient in surface sediment or deep sediment, respectively.

To comprehensively and quantitatively assess the concentration effect of sulfate on the internal P release in natural eutrophic waters (for instance, Lake Taihu in China), four linear regression equations were established, based on the functional relationships between the apparent fluxes (F_1, F_0 of labile Fe and P) and the concentrations of sulfate in overlying water. In addition, we extended the applied scope of the regression equations to predict the change of apparent fluxes of labile Fe and P over a wider concentration range of sulfate in freshwater systems. Here, four critical values for sulfate were determined by equations according to the following two scenarios:

Scenario 1: When the apparent diffusive flux of labile P or labile Fe across the SWI was zero ($F_0=0$)

Scenario 2: When the apparent diffusive fluxes of labile P or labile Fe were equal at the SWI and at 1 cm below the SWI ($F_{10}=F_1-F_0$).

Based on the four critical values of sulfate derived here, we selected two of the critical values, which did not belong to the concentration range (~3,000-30,000 μM) of salt waters (Caraco et al. 1989) and divided the concentration range (0-3,000 μM) into different parts.

All of the statistical analyses were performed using SPSS software (*V25.0*; SPSS, USA). The differences of DO, Eh, SRP in overlying water and oxygen penetration depth (OPD) in sediment between different treatments were determined by pairwise

275 comparisons using one-way analysis of variance (ANOVA) and the Duncans multiple

276 range test were used to perform means comparison. Besides, the differences of labile S,

277 labile Fe and labile P between different sampling times were also assessed. The

278 differences between the mean values at significance probability (p)<0.05 were

279 considered statistically significant. ~~One-way analysis of variance (ANOVA) was~~

280 ~~employed to detect differences of DO, Eh, SRP in overlying water and oxygen~~

281 ~~penetration depth (OPD) in sediment between different treatments. The difference of~~

282 ~~labile S, labile Fe and labile P between different sampling times were also assessed by~~

283 ~~ANOVA. A P<0.05 was considered significant.~~ The functional relationships between

284 sulfate concentration in the overlying water and fluxes of labile Fe and P were

285 established using linear fitting.

3. Results

3.1. Vertical distribution of DO and Eh in sediment-water interface

288   Sulfate addition induced an apparent change in the DO profiles, including DO level

289 (Figure.1a.) and DO penetration depth (Figure.2a) in the surficial sediment. The highest

290 DO concentrations in bottom water and at each depth along the vertical water-sediment

291 profiles were always found in the group A. The sediment oxygen concentrations in the

292 group B were also higher at depths of -0.05 to -0.7 cm than those in the Control

293 (Figure.1a). Furthermore, higher sulfate concentrations led to a significant increase in

294 the vertical oxygen penetration depth (OPD) in the order of group A>group B>Control

295 (one-way ANOVA, p<0.05) (Figure.2b).

296   The redox potential (ORP) showed a similar trend to DO (Figure.1b, Figure.2c).

297   Sulfate addition significantly increased the ORP values in bottom water and followed

298   the order group A>group B>Control (one-way ANOVA, $p<0.05$). From the SWI to the

299   depth of -3 cm, the ORP values in the group A and group B units were significantly

300   higher than those in the Control group (one-way ANOVA, $p<0.05$).
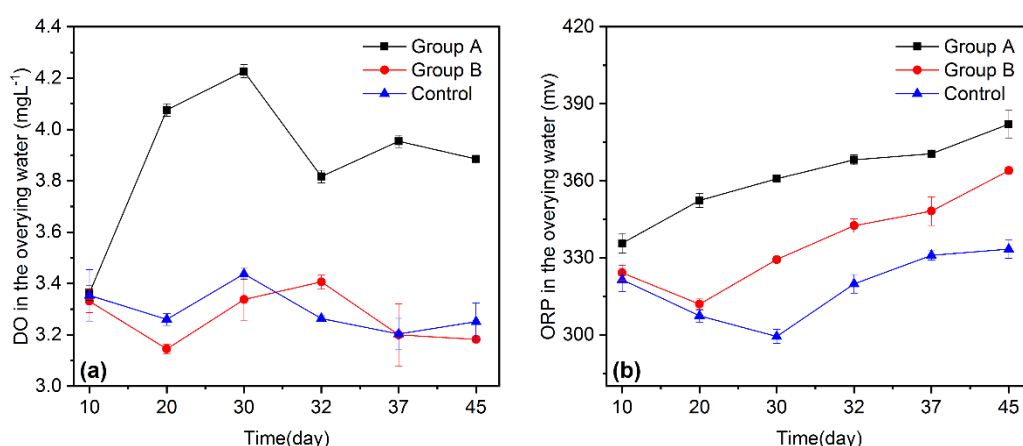

302   Figure 1. Variation of dissolved oxygen (DO) (a) and redox potential (ORP) (b) in bottom water

303   from the three treatment groups during the 45-days incubation (data shown by mean ± SD, n =

304   2). Control: 970 μM; group B: low sulfate, 1,770 μM; group A: high sulfate, 2,600 μM.
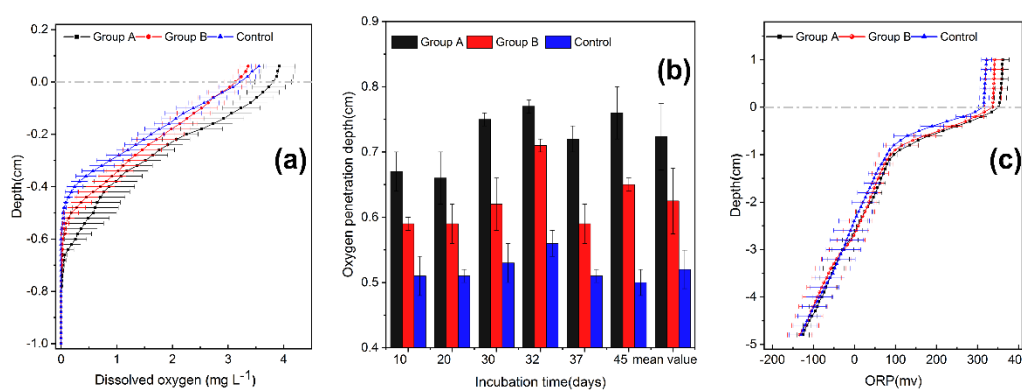
306   Figure 2. Dissolved oxygen profiles (DO) (a), oxygen penetration depth (OPD) (data shown by

307   mean ± SD, n = 2) (b) and redox potential (ORP) profiles (c) form the three treatment groups

308   (data of DO and OPD were shown by the mean values during the 45-days incubation period ±

309   SD, n=12). The horizontal dashed line indicates the sediment-water interface (SWI). Control:

310   970 μM; group B: low sulfate, 1,770 μM; group A: high sulfate, 2,600 μM.

3.2. Vertical distribution of sulfate and DGT-labile S in the sediment-water profiles

312   The concentrations of sulfate in overlying water were 2,394±67 in group A,

313   1,658±33 in group B, and 911±55 μM in the Control (Figure. 3a). In all groups, the

314   sulfate concentration in pore water decreased slightly with increase in sediment depth.

315   In addition, the concentration of sulfate in pore water at each depth followed the order

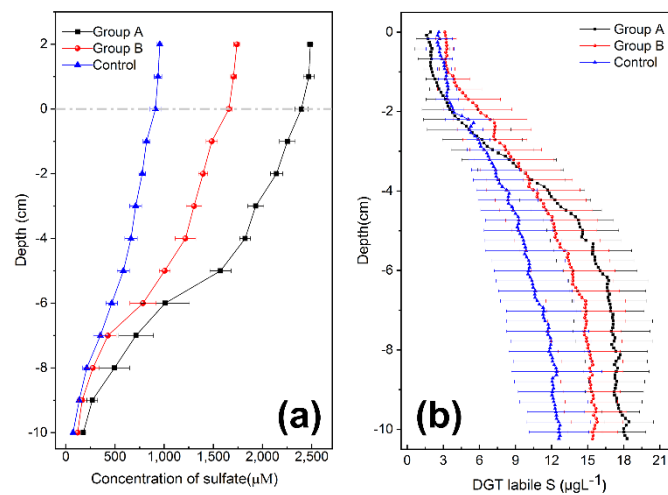316   group A>group B>Control (Figure. 3a).

317

318   Figure 3. Changes in the concentration of sulfate with depth in the sediment-overlying water

319   profiles (a) (data of sulfate was shown by the mean values of all sampling times during the 45-

320   days incubation period ±SD, n=12), one-dimensional distributions of DGT-labile S in profiles

321   as determined by AgI DGT (b) of different sulfate treatments (the data of labile S was shown

322   by the mean values of all sampling times during the 45-days incubation period ± SD, n=6). The

323   horizontal dashed line indicates SWI. Control: 970 μM; group B: low sulfate, 1,770 μM; group

324   A: high sulfate, 2,600 μM.

325   The labile S (Figure.3b) profiles exhibited a similar trend, increasing with depth in

326   all three groups. Interestingly, lower concentrations of labile S in surface sediments

327   were found in group A, except at day 20 (Figure.S4). The average concentrations of

328   labile S within the depths from SWI to -3 cm in group A were lower than those in the

329   Control and group B (Figure.3b). However, that trend was reversed below -4 cm. The

330   concentration of labile S in group A remained at a higher level in the deep sediment

331   (below -3 to -4 cm) throughout the incubation period (Figure.S4). The average

332   concentrations of labile S in group A from -4 to -10 cm were significantly higher than

333   those in group B and the Control (one-way ANOVA, $p<0.05$).

334   *3.3. Vertical distribution of SRP in sediment-water profiles*

335   Soluble reactive P (SRP) concentrations in the overlying water were significantly

336   higher in the groups with the increasing sulfate concentration (one-way ANOVA,

337    $p<0.05$) and the average values followed the order: group A>group B>Control (Figure.

338   4 and Figure. S3). After the 30th day of incubation, the concentration of SRP in the pore

339   water of sulfate addition groups (group A and B) was higher than the Control. On the

340   45th day of incubation, the average concentrations of SRP in pore water from SWI to -

341   8 cm in group A and group B were 52.3% and 48.6% higher than the Control. However

342   below -8 cm, no evident difference in concentrations of SRP was observed during 45-

343   days incubation between the three groups (RSD=1.06 % in three groups).
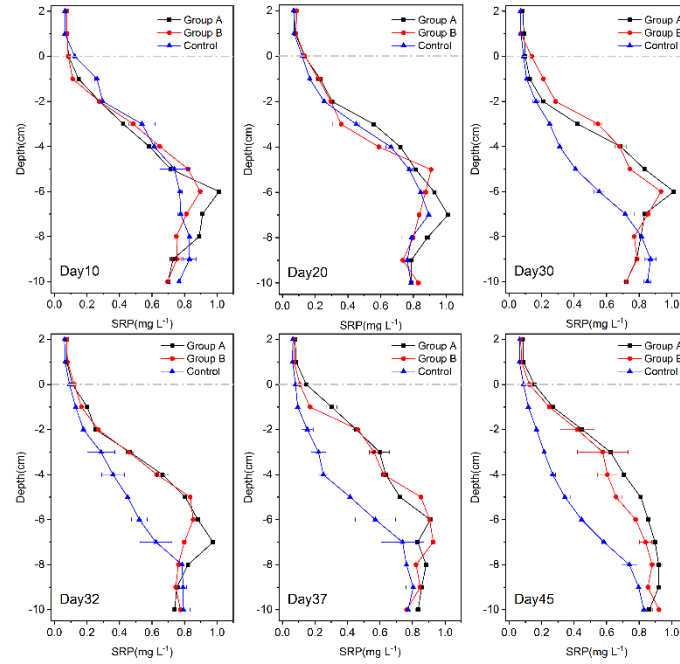
Figure 4. Changes of SRP (Soluble Reactive P) in the sediment-water profiles from the three treatment groups during the 45-days incubation period (data shown by mean ± SD, n = 2).The horizontal dashed line indicates the SWI. Control: 970 μM; group B: low sulfate, 1,770 μM; group A: high sulfate, 2,600 μM.

3.4. Vertical distribution of DGT-labile Fe and P in sediment-water profile

The concentrations of labile Fe and P from the overlying water to the surface sediments (SWI to -1cm) remained at relatively low values and increased until -10 cm sediment depth (Figure.5, Figure.S5 and Figure.S6). There was no significant difference for labile Fe and labile P between different sampling time (most of P >0.05, the specific *P* values were listed in Table S2 and Table S3). Below -1cm, the concentrations of labile Fe were varied from 0.24 to 2.71 mg L^{-1} in group A, 0.13 to 2.82 mg L^{-1} in group B and 0.10 to 3.21 mg L^{-1} in the Control group, respectively. However, the concentrations of labile P were ranged between 0.01 to 0.33 mg L^{-1} in group A, 0.03 to 0.30 mg L^{-1} in group B and 0.01 to 0.28 mg L^{-1} in the Control.

18

359   Statistically significant positive correlations between labile Fe and labile P in sediment

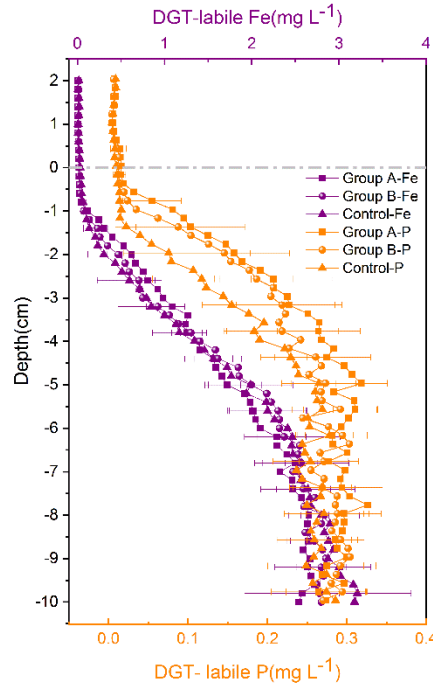360   were determined for each treatment (p< 0.001) (Fig.S7).

361

362   Figure 5. Effects of the sulfate addition on the one-dimensional vertical distribution of DGT-

363   labile P and DGT-labile Fe in water-sediments profiles (data shown by the mean values of all

364   sampling times during the 45-days incubation period ± SD, n=6). The horizontal dashed line

365   indicates the sediment-water interface (SWI). Control: 970 μM; group B: low sulfate, 1,770

366   μM; group A: high sulfate, 2,600 μM.

367   *3.5. Apparent diffusive flux of PO_4^{3-} and Fe(II)*

368   The apparent diffusive fluxes of the target elements were calculated at SWI (F_0) and

369   1 cm below the SWI (F_1) based on Fick`s first law (Figure. 6). The apparent fluxes of

370   PO_4^{3-} and Fe(II) in the three groups across the SWI were all positive (effluxes) and

371   ranged between 0.06 to 4.56 mgm^{-2}d^{-1} and 1.41 to 5.32 mgm^{-2}d^{-1}, respectively. The

372   mean flux of PO_4^{3-} from the surface layer of sediment to water (F_0) showed an

373   increasing trend with the increase of sulfate in overlying water. The mean F_0 of PO_4^{3-}

374   in group A and group B were 5.5 and 1.9 times higher than that in the Control (0.40

375    $mgm^{-2}d^{-1}$), respectively. The mean F_0 of Fe(II) was lowest in group A (2.22 $mgm^{-2}d^{-1}$)

376   compared to that in group B (2.67 $mgm^{-2}d^{-1}$) and the Control (3.51 $mgm^{-2}d^{-1}$). The

377   values of F_1 in three groups were also positive and the fluxes of PO_4^{3-} and Fe(II) from

378   deep sediment to surface sediment ranged between 0.88 to 4.00 $mgm^{-2}d^{-1}$ and 8.24 to

379   30.53 $mgm^{-2}d^{-1}$. Increasing sulfate in overlying water elevated the mean values of the

380   flux of PO_4^{3-} from deep sediment to surface sediment (F_1) with order of group A>group

381   B>Control, whereas an opposite trend was observed for Fe(II).

382   The net flux (F_{10}) of PO_4^{3-} and Fe(II) in the surface sediment was calculated by

383   using the equation: $F_{10}=F_1-F_0$. The F_{10} of PO_4^{3-} and Fe(II) were all positive, except for

384   F_{10} of P in group A (highly variable, from 0.88 to -0.48 $mgm^{-2}d^{-1}$). The mean values of

385   F_{10} decreased with the increased sulfate in the overlying water. The retention

386   efficiencies (defined by the quotient of F_1 and F_{10}) of P, diffused from deep to surface

387   sediments in the Control group was about 70.1% and obviously higher than those in the

388   group A and group B groups (3.6% and 22.1%, respectively). The retention efficiencies

389   of Fe(II) were 78.5%, 80.4% and 80.8% in group A, group B and C, respectively.
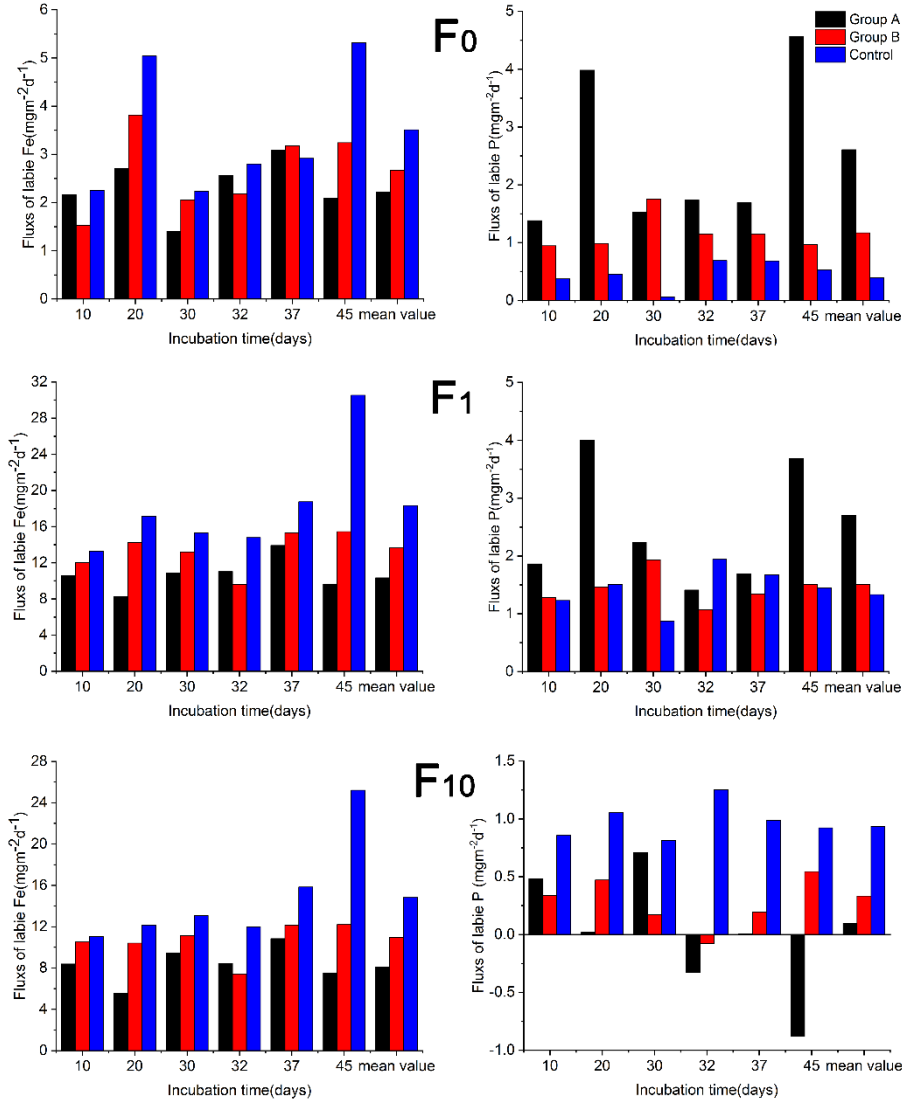
Figure. 6 the apparent diffusive fluxes of PO_4^{3-} and Fe^{2+} in different treatments. The label F_0 represents the diffusive flux of PO_4^{3-} and Fe^{2+} from surface sediments to water. F_1 represents the diffusive flux of PO_4^{3-} and Fe^{2+} from deep to surface sediments. F_{10} ($F_{10}=F_1-F_0$) is net flux of PO_4^{3-} and Fe^{2+} in surface sediment. The mean flux of each group represents the average flux during the 45-days incubation period. The mean values of fluxes given here were calculated according to the following equation: $\overline{F} = \dfrac{\sum_{i=1}^{6}(F_i \times t_i)}{\sum_{i=1}^{6} t_i}$

Where $\overline{F}$ is the average flux during the 45-days incubation (mg m^{-2} d^{-1}), F_i is the flux on the ith sampling day (mgm^{-2} d^{-1}), t_i is the time interval from the (i-1)th sampling day to the ith sampling day (day). Control: 970 μM; group B: low sulfate, 1,770 μM; group A: high sulfate, 2,600 μM.

21

401　*3.6. Relationship between sulfate concentration and internal P release*

402　　　Based on the fluxes of labile Fe and P at six sampling times across the SWI (F_0) and

403　1 cm below the SWI (F_1), we constructed the diagram for sulfate (Figure. 7). The fluxes

404　of labile P from deep to surface sediments (F_1) were all positive. Furthermore, a 100

405　μM increase of sulfate in overlying water, compared to the concentration of sulfate in

406　the Control group, would induce a 0.128 mgm^{-2}d^{-1} increase of P flux from surface

407　sediment to the overlying water (Figure. S8).

408　　　When the concentrations of sulfate were less than 646 μM (Part I in the diagram),

409　the flux of labile P across the SWI was negative. When the concentration increased

410　from 646 to 2,375 μM (Part II), the difference between F_1 and F_0 of labile P gradually

411　reduced to zero. When the concentration of sulfate further increased to more than 2,375

412　μM (Part III), F_0 of labile P was larger than F_1. The flux of labile Fe at two depths, over

413　the whole concentration range of sulfate (0 to 3,000 μM), were all positive and F_0 was

414　always less than F_1. In addition, the difference between F_0 and F_1 of labile Fe

415　continuously decreased with the increase of sulfate in overlying water.
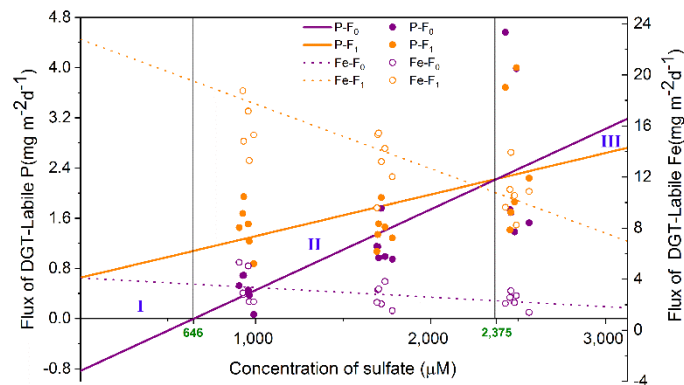

416

417　Figure. 7. The functional relation between the apparent diffusive fluxes of PO_4^{3-}(Fe^{2+}) and

418　sulfate in overlying water within a concentration range of 0-3,000 μM. The label **F_0** represents

419   the diffusive flux of PO_4^{3-} and Fe^{2+} from surface sediment to overlying water and $\mathbf{F_1}$ represents

420   the diffusive flux from deep to surface sediments.

421   ## 4. Discussion

422   *4.1. Effects of sulfate elevation on the internal P release*

423   It has been reported that elevated sulfate concentrations in freshwaters systems with

424   intermediate concentrations of sulfate (>100 μM), greatly promoted the release of

425   internal P under anoxic conditions (Caraco et al. 1989, 1993, Chen et al. 2016a). As for

426   under oxic conditions, Zak et al. (2006) found that increasing sulfate affected the

427   mobilization of P in a lowland freshwater river polluted by mining activities with

428   extremely high concentrations of sulfate (2,600-7,800 μM). Those concentrations of

429   sulfate are typical of the concentration range (~3,000-30,000 μM) of salt waters (Caraco

430   et al. 1989). Here, we additionally found that sulfate with modest concentrations (970-

431   2,600 μM) promoted release of P under oxic conditions across the SWI.

432   A higher concentration of SRP in the overlying water was observed with an increase

433   in sulfate (Figure. 4 and Figure. S3). At the end of experiment, the mean concentrations

434   of SRP in sediment pore water from the SWI to -8 cm were 52.3% and 48.6% greater

435   in the group A and group B, respectively, when compared to the Control group (Figure.

436   4). In addition, P fluxes at the SWI were all positive, which suggested that P was

437   released from surface sediments to the water column (Figure.6). P fluxes from deep to

438   surface sediments (Figure.6) were also positive (F_1 of P >0) and larger than the

439   corresponding fluxes from surface sediment to water, indicating that P released from

440   the oxic surface sediment mainly originated from deeper sediment. Compared with our

441   results under oxic conditions, the maximum concentration of SRP in overlying water

442   under anoxic environments was one order of magnitude higher and the released P was

443   mainly from surface sediments (Chen et al. 2016a, Han et al. 2015). These results

444   demonstrated that redox conditions clearly influenced the mechanisms of sulfate-

445   promoted release of internal P.

446   *4.2. Mechanisms of sulfate-promoted release of internal P*

447   The process of sulfate-promoted internal P release is closely linked to the reduction

448   of sulfate in sediments (Caraco et al. 1989, Roden and Edmonds 1997, Rozan et al.

449   2002, Zak et al. 2006). Higher concentrations of labile S below -3cm (Figure. 3b) were

450   observed in group A, which can be mainly attributed to the increase of sulfate in

451   overlying water triggering more sulfate penetration and reduction in the deep sediment.

452   The fluxes of P from deep to surface sediments increased along with the increase of

453   sulfate in water column (Figure. 6). This result agreed well with the previous report that

454   P mobilization is ultimately dependent on the concentration of S(-II) (Zhao et al. 2019).

455   Usually, the source of sulfide is mainly controlled by the reduction of sulfate (Motelica-

456   Heino et al. 2003), which, in freshwater sediments, is regulated by many factors, such

457   as dissolved oxygen, organic matter and concentration of sulfate (Leonov and

458   Chicherina 2008). Here, below the depth of -1 cm, oxygen was exhausted (Figure. 2a)

459   and ORP values decreased to <100 mV (Figure. 2c) in all three groups, which suggested

460   that deep sediment became anoxic and conditions were suitable for sulfate reduction.

461   The rate of sulfate reduction has been reported as a diffusion-limited, first-order rate

462   process and dependent on initial sulfate concentration (Loh et al. 2013). In our study,

463   increasing concentrations of sulfate in the overlying water led to higher concentrations

464   of sulfate in the pore water (Figure. 3a), which may have accounted for the enhanced

465   activity of sulfate reduction in the deeper, anoxic layers of sediment.

466   In addition to influencing sulfate reduction in the sediments, higher concentrations

467   of sulfate in the overlying water will also influence the dynamics of Fe(II) in the

468   sediment (Figure. 6). The positive correlations (p<0.001) between labile Fe(II) and

469   labile P (Figure.S7) in each treatment that suggested coincident distributions of labile

470   Fe and labile P existed in the sediment. These coincident distributions with depth should

471   be a result of the reduction of the P-bearing Fe(III)(oxyhydr)oxides (Ding et al. 2012,

472   Xu et al. 2012). The reduction of Fe(III)(oxyhydr)oxides in sediments to Fe(II), is a

473   basic pattern for the P mobilization from sediment to water (Christophoridis and

474   Fytianos 2006). The Fe(II) produced can be maintained in the deep sediment through

475   the formation as iron sulfide coupled with sulfate reduction (Roden and Edmonds 1997).

476   For instance, even under sulfate concentrations limited to 200 μM, sulfide-mediated

477   chemical iron reduction (SCIR) in freshwater systems is a dominate pathway of iron

478   reduction (Hansel et al. 2015). The reduced Fe(II) could precipitate as sulfides via SCIR

479   or directly react with S(-II) in the pore water other than getting back into pore water

480   (Kwon et al. 2014, Lehtoranta et al. 2009). These coincide with our observations that

481   the concentration range of labile Fe (Figure. 5) and fluxes of labile Fe from deep

482   sediment to surface sediment (Figure. 6) were both decreased in high sulfate system

483   (group A) under a higher concentration of S(-II). Thus, the upward diffusive fluxes of

484   Fe(II) from deep to surface sediments in high sulfate systems were reduced by enhanced

485   sulfate reduction. This resulted in less Fe(II) and sulfide diffusing to the surface

486   oxidized layer as Fe(II) precipitation as sulfides occurred in the deep sediments.

487   Therefore, fewer reducing substances would consume oxygen already present in

488   sediment in High sulfate systems, supporting the observation that a better-oxidized

489   condition existed in surface sediments and that higher DO concentrations across the

490   SWI were found in group A and group B systems compared to the Control (Figure. 2a).

491   In this study, the oxygen penetration depth (OPD) varied from 0.48 to 0.78 cm

492   (Figure.2b), suggesting that an oxidized layer existed in the surface sediment. Under

493   natural conditions, a thin oxidized layer may exist in surficial sediment in shallow

494   waters, where it can easily be further oxygenated by hydrodynamic disturbance

495   (Chatelain and Guizien 2010). Oxic conditions are important for iron to maintain its

496   oxidized state, which, in turn, correlates with P retention in sediments (Mortimer 1942).

497   The OPD regulates the thickness of the oxic layer (Wang et al. 2014), a higher thickness

498   decreasing the P release from sediment to overlying water (McManus et al. 1997).

499   However, a higher concentration of SRP released from surface sediment to water was

500   observed in the High sulfate (group A) system (Figure. 4 and Figure. 6). These results

501   suggested that even the deeper OPD of around several millimeters might not be enough

502   to retain the excessive P released from sediment to water induced by elevated sulfate.

503   Most of the upward diffused Fe(II) in each group (retention efficiencies of Fe(II)

504   varied from 78.5% to 80.8%) was oxidized and retained in surface sediment (Figure. 6)

505   as the oxidation of Fe(II) by oxygen is a rapid process (Chen et al. 2015). Lower fluxes

506   of Fe(II) from deep to surface sediment in the higher sulfate level systems resulted in a

507   lower P-retaining capacity in surface sediments. The decreased ratio of labile Fe to P in

508   sediment associated with higher sulfate also suggested higher sulfate lowered the P

509   retaining capacity (Figure. S7). Therefore, the fluxes of Fe(II), rather than oxygen, were

510   responsible for the larger release of P in more concentrated sulfate systems.

511   *4.3. Concentration effect of sulfate on internal P release*

512   In this study, we found that increasing sulfate could promote internal P release in

513   eutrophic waters and have the potential to switch sediments between P source and sink,

514   if factors other than sulfate concentration are not considered (Figure.7). The control of

515   P and sulfate concentration in water were both necessary. Thus, it is important to

516   quantify the effects of sulfate concentration on internal P release under oxic conditions

517   across the SWI in any given freshwater system.

518   That the fluxes of P from deep to surface sediments were all positive (F_1 of P>0)

519   suggesting that, in some eutrophic waters, P release from deep sediments might be

520   inevitable. When concentrations of sulfate were lower than 646 μM, well-oxidized

521   conditions across the SWI would be effective for sediment retention of P (F_0 of P<0).

522   However, at sulfate levels >646 μM, a 100 μM increase of sulfate in overlying water

523   would result in a 0.128 mgm^{-2}d^{-1} increase in P flux from the sediment to the water

524 column. In this case, just maintaining a thin oxidized layer (<1 cm) in surface sediment

525 would not be sufficient to control internal P release, as enhanced sulfate reduction

526 limited the Fe(II) release from deep to surface sediments. Once sulfate increased to

527 more than 2,375 μM, the retention capacity for P in the oxidized layer would be

528 exhausted and surface sediment would become another source of P to be released to

529 overlying water. Furthermore, increasing concentrations of sulfate, would gradually

530 reduce the upward diffusion of Fe(II) from the deep sediment, decreasing the

531 production of new adsorption sites for P in surface sediments.

532 *4.4. Environmental implications*

533 Previous studies reporting that sulfate could induce the release of P from sediment

534 mainly focused on anoxic conditions (Caraco et al. 1993, Chen et al. 2016a, Han et al.

535 2015, Roden and Edmonds 1997). However, a thin oxidized layer usually exists in

536 surficial sediments in shallow waters and anoxic conditions might not persist during

537 most seasons except over the algal bloom period. In this study, we found that, under

538 oxic conditions across the SWI with modest concentrations of sulfate in eutrophic

539 freshwater, increasing sulfate levels could also promote the release of P from the

540 sediment. The release of internal P induced by sulfate under oxic conditions across the

541 SWI was one magnitude less than in anoxic environments. However, as cyanobacteria

542 have a higher affinity for P, situations with these low concentrations and continuously-

543 released phosphorus from sediment may still contribute to eutrophication and even

544 production of algal blooms (Prentice et al. 2015). Sediments served as a source for the

P supply in the water column used by cyanobacteria, and such a process was activated greatly by the higher concentration of sulfate, which pumped up more P from the sediments. More importantly, the intensity of P release was directly influenced by the concentration of sulfate in overlying water and the flux of Fe(II) was the primary factor responsible for P retention. Therefore, as oxygen penetration depth in natural sediments is limited, just improving or maintaining the oxygen level in bottom water may alone be insufficient ~~to control internal P release in a high sulfate ecosystem~~. Technologies aim to increase the depth of oxygen penetration in sediment, suppress the sulfate reduction, or provide new adsorption sites in sediment would be promising for the control internal P release in a high sulfate ecosystem.

5. Conclusions

This study investigated the effect of increasing sulfate in shallow waters on internal P release under oxic conditions across the SWI. Higher concentrations of sulfate increased the concentration of SRP in both overlying and pore waters. In addition, higher concentrations of sulfate in overlying water induced a significant increase of labile S(-II) in deep sediment, indicating that enhanced sulfate penetration and reduction occurred in deeper layers of sediment. The fluxes of labile Fe and P from deep to surface sediments were positive and greater than the corresponding fluxes from surface sediment to water column, suggesting that reduction of P-bearing Fe(III)(oxyhydr)oxides in deep sediment acted as a major source for internal P release under oxic conditions across the SWI. Lower fluxes of Fe(II) from deep to surface

566   sediments were found in the High sulfate experimental system, resulting in less re-

567   oxidized Fe(III) in surface sediments. However, induced by the elevated sulfate, more

568   P released from deep sediment to surface sediment inevitably resulted in an increase in

569   the flux of P across the SWI. The results indicated that the influence of sulfate on

570   internal P released depended largely on the concentrations of sulfate. When the

571   concentration of sulfate was larger than ca. 646 μM, a 100 μM increase of sulfate

572   induced a 0.128 $mgm^{-2}d^{-1}$ increase of P flux from surface sediment to water column.

573   Therefore, sulfate concentrations should be considered and controlled for the

574   management of eutrophic waters.

Acknowledgements

References

580   Bostrom, B., Andersen, J.M., Fleischer, S. and Jansson, M. (1988) Exchange of Phosphorus

581   across the Sediment - Water Interface. Hydrobiologia 170, 229-244.

582   Caraco, N.F., Cole, J.J. and Likens, G.E. (1989) Evidence for Sulfate-Controlled Phosphorus

583   Release from Sediments of Aquatic Systems. Nature 341(6240), 316-318.

584   Caraco, N.F., Cole, J.J. and Likens, G.E. (1993) Sulfate Control of Phosphorus Availability in

585   Lakes - a Test and Reevaluation of Hasler and Einsele Model. Hydrobiologia 253(1-3), 275-

586   280.

587   Carpenter, S.R. (2008) Phosphorus control is critical to mitigating eutrophication. Proceedings

588   of the National Academy of Sciences of the United States of America 105(32), 11039-11040.

589   Chatelain, M. and Guizien, K. (2010) Modelling coupled turbulence - Dissolved oxygen

590   dynamics near the sediment-water interface under wind waves and sea swell. Water

591   Research 44(5), 1361-1372.

592   Chen, M., Ding, S., Liu, L., Xu, D., Han, C. and Zhang, C. (2015) Iron-coupled inactivation of

593   phosphorus in sediments by macrozoobenthos (chironomid larvae) bioturbation: Evidences

594   from high-resolution dynamic measurements. Environmental Pollution 204, 241-247.

595   Chen, M., Li, X.H., He, Y.H., Song, N., Cai, H.Y., Wang, C.H., Li, Y.T., Chu, H.Y., Krumholz,

596   L.R. and Jiang, H.L. (2016a) Increasing sulfate concentrations result in higher sulfide

597   production and phosphorous mobilization in a shallow eutrophic freshwater lake. Water

598   Research 96, 94-104.

599   Chen, M.S., Ding, S.M., Liu, L., Xu, D., Gong, M.D., Tang, H. and Zhang, C.S. (2016b)

600   Kinetics of phosphorus release from sediments and its relationship with iron speciation

601   influenced by the mussel (Corbicula fluminea) bioturbation. Science of the Total

602   Environment 542, 833-840.

603   Christophoridis, C. and Fytianos, K. (2006) Conditions affecting the release of phosphorus from

604   surface lake sediments. Journal of Environmental Quality 35(4), 1181-1192.

605   Conley, D.J., Paerl, H.W., Howarth, R.W., Boesch, D.F., Seitzinger, S.P., Havens, K.E.,

606   Lancelot, C. and Likens, G.E. (2009) ECOLOGY Controlling Eutrophication: Nitrogen and

607 Phosphorus. Science 323(5917), 1014-1015.

608 Coveney, M.F., Lowe, E.F., Battoe, L.E., Marzolf, E.R. and Conrow, R. (2005) Response of a

609 eutrophic, shallow subtropical lake to reduced nutrient loading. Freshwater Biology 50(10),

610 1718-1730.

611 Ding, S., Han, C., Wang, Y., Yao, L., Wang, Y., Xu, D., Sun, Q., Williams, P.N. and Zhang, C.

612 (2015) In situ, high-resolution imaging of labile phosphorus in sediments of a large

613 eutrophic lake. Water Research 74, 100-109.

614 Ding, S.M., Sun, Q., Xu, D., Jia, F., He, X. and Zhang, C.S. (2012) High-Resolution

615 Simultaneous Measurements of Dissolved Reactive Phosphorus and Dissolved Sulfide: The

616 First Observation of Their Simultaneous Release in Sediments. Environmental Science &

617 Technology 46(15), 8297-8304.

618 Gächter, R. and Müller, B. (2003) Why the Phosphorus Retention of Lakes Does Not

619 Necessarily Depend on the Oxygen Supply to Their Sediment Surface. Limnology &

620 Oceanography 48(2), 929-933.

621 Gao, Y., Liang, T., Tian, S., Wang, L., Holm, P.E. and Hansen, H.C.B. (2016) High-resolution

622 imaging of labile phosphorus and its relationship with iron redox state in lake sediments.

623 Environmental Pollution 219, 466-474.

624 Han, C., Ding, S.M., Yao, L., Shen, Q.S., Zhu, C.G., Wang, Y. and Xu, D. (2015) Dynamics of

625 phosphorus-iron-sulfur at the sediment-water interface influenced by algae blooms

626 decomposition. Journal of Hazardous materials 300, 329-337.

627 Hansel, C.M., Lentini, C.J., Tang, Y.Z., Johnston, D.T., Wankel, S.D. and Jardine, P.M. (2015)

628   Dominance of sulfur-fueled iron oxide reduction in low-sulfate freshwater sediments. Isme

629   Journal 9(11), 2400-2412.

630   Higashino, M. (2011) Oxygen consumption by a sediment bed for stagnant water: Comparison

631   to SOD with fluid flow. Water Research 45(15), 4381-4389.

632   Huser, B.J., Futter, M.N., Wang, R. and Fölster, J. (2018) Persistent and widespread long-term

633   phosphorus declines in Boreal lakes in Sweden. Science of the Total Environment 613-614,

634   240-249.

635   Jilbert, T., Slomp, C.P., Gustafsson, B.G. and Boer, W. (2011) Beyond the Fe-P-redox

636   connection: preferential regeneration of phosphorus from organic matter as a key control

637   on Baltic Sea nutrient cycles. Biogeosciences 8(6), 1699-1720.

638   Kraal, P., Burton, E.D., Rose, A.L., Cheetham, M.D., Bush, R.T. and Sullivan, L.A. (2013)

639   Decoupling between Water Column Oxygenation and Benthic Phosphate Dynamics in a

640   Shallow Eutrophic Estuary. Environmental Science & Technology 47(7), 3114-3121.

641   Kwon, M.J., Boyanov, M.I., Antonopoulos, D.A., Brulc, J.M., Johnston, E.R., Skinner, K.A.,

642   Kemner, K.M. and O'Loughlin, E.J. (2014) Effects of dissimilatory sulfate reduction on

643   FeIII (hydr)oxide reduction and microbial community development. Geochimica et

644   Cosmochimica Acta 129, 177-190.

645   Lehtoranta, J., Ekholm, P. and Pitkanen, H. (2009) Coastal Eutrophication Thresholds: A Matter

646   of Sediment Microbial Processes. Ambio 38(6), 303-308.

647   Leonov, A.V. and Chicherina, O.V. (2008) Sulfate reduction in natural water bodies. 1. The

648   effect of environmental factors and the measured rates of the process. Water Resources

649   35(4), 417-434.

650   Li, Y.H. and Gregory, S. (1974) DIFFUSION OF IONS IN SEA-WATER AND IN DEEP-SEA

651   SEDIMENTS. Geochimica et Cosmochimica Acta 38(5), 703-714.

652   Loh, P.S., Molot, L.A., Nuernberg, G.K., Watson, S.B. and Ginn, B. (2013) Evaluating

653   relationships between sediment chemistry and anoxic phosphorus and iron release across

654   three different water bodies. Inland Waters 3(1), 105-118.

655   McManus, J., Berelson, W.M., Coale, K.H., Johnson, K.S. and Kilgore, T.E. (1997) Phosphorus

656   regeneration in continental margin sediments. Geochimica et Cosmochimica Acta 61(14),

657   2891-2907.

658   Mortimer, C.H. (1942) The exchange of dissolved substances between mud and water in lakes.

659   Journal of Ecology 30, 147-201.

660   Motelica-Heino, M., Naylor, C., Zhang, H. and Davison, W. (2003) Simultaneous release of

661   metals and sulfide in lacustrine sediment. Environmental Science & Technology 37(19),

662   4374-4381.

663   Murphy, J. and Riley, J.P. (1962) A modified single solution method for the determination of

664   phosphate in natural waters. Analytica Chimica Acta 27, 31-36.

665   Paerl, H.W., Hall, N.S. and Calandrino, E.S. (2011) Controlling harmful cyanobacterial blooms

666   in a world experiencing anthropogenic and climatic-induced change. Science of the Total

667   Environment 409(10), 1739-1745.

668   Paytan, A., Roberts, K., Watson, S., Peek, S., Chuang, P.C., Defforey, D. and Kendall, C. (2017)

669   Internal loading of phosphate in Lake Erie Central Basin. Science of the Total Environment

670   579, 1356-1365.

671   Prentice, M.J., OBrien, K.R., Hamilton, D.P. and Burford, M.A. (201 5) High- and low-affinity

672   phosphate uptake and its effect on phytoplankton dominance in a phosphate-depauperate

673   lake. Aquatic Microbial Ecology 75(2), 139-153.

674   Qin, B.Q., Xu, P.Z., Wu, Q.L., Luo, L.C. and Zhang, Y.L. (2007) Environmental issues of Lake

675   Taihu, China. Hydrobiologia 581, 3-14.

676   Roden, E.E. and Edmonds, J.W. (1997) Phosphate mobilization in iron-rich anaerobic

677   sediments: Microbial Fe(III) oxide reduction versus iron-sulfide formation. Archiv Fur

678   Hydrobiologie 139(3), 347-378.

679   Rozan, T.F., Taillefert, M., Trouwborst, R.E., Glazer, B.T., Ma, S.F., Herszage, J., Valdes, L.M.,

680   Price, K.S. and Luther, G.W. (2002) Iron-sulfur-phosphorus cycling in the sediments of a

681   shallow coastal bay: Implications for sediment nutrient release and benthic macroalgal

682   blooms. Limnology and Oceanography 47(5), 1346-1354.

683   Rydin, E. (2000) Potentially mobile phosphorus in Lake Erken sediment. Water Research 34(7),

684   2037-2042.

685   Schindler, D.W., Hecky, R.E., Findlay, D.L., Stainton, M.P., Parker, B.R., Paterson, M.J., Beaty,

686   K.G., Lyng, M. and Kasian, S.E.M. (2008) Eutrophication of lakes cannot be controlled by

687   reducing nitrogen input: Results of a 37-year whole-ecosystem experiment. Proceedings of

688   the National Academy of Sciences of the United States of America 105(32), 11254-11258.

689   Smith, V.H. (2003) Eutrophication of freshwater and coastal marine ecosystems - A global

690   problem. Environmental Science and Pollution Research 10(2), 126-139.

691   Sun, Q., Ding, S.M., Zhang, L.P., Chen, M.S. and Zhang, C.S. (2017) A millimeter-scale

692   observation of the competitive effect of phosphate on promotion of arsenic mobilization in

693   sediments. Chemosphere 180, 285-294.

694   Tabatabai, M.A. (1974) A Rapid Method for Determination of Sulfate in Water Samples.

695   Environmental Letters 7(3), 237-243.

696   Tong, Y., Zhang, W., Wang, X., Couture, R.M., Larssen, T., Zhao, Y., Li, J., Liang, H., Liu, X.

697   and Bu, X. (2017) Decline in Chinese lake phosphorus concentration accompanied by shift

698   in sources since 2006. Nature Geoscience 10(7), 12-2017.

699   Ullman, W.J. and Aller, R.C. (1982) Diffusion-Coefficients in Nearshore Marine-Sediments.

700   Limnology and Oceanography 27(3), 552-556.

701   Wang, C., Shan, B., Zhang, H. and Rong, N. (2014) Analyzing sediment dissolved oxygen

702   based on microprofile modeling. Environmental Science and Pollution Research 21(17),

703   10320-10328.

704   Wang, Y., Ding, S.M., Wang, D., Sun, Q., Lin, J., Shi, L., Chen, M.S. and Zhang, C.S. (2017)

705   Static layer: A key to immobilization of phosphorus in sediments amended with lanthanum

706   modified bentonite (Phoslock (R)). Chemical Engineering Journal 325, 49-58.

707   Xu, D., Chen, Y.F., Ding, S.M., Sun, Q., Wang, Y. and Zhang, C.S. (2013) Diffusive Gradients

708   in Thin Films Technique Equipped with a Mixed Binding Gel for Simultaneous

709   Measurements of Dissolved Reactive Phosphorus and Dissolved Iron. Environmental

710   Science & Technology 47(18), 10477-10484.

711   Xu, D., Wu, W., Ding, S.M., Sun, Q. and Zhang, C.S. (2012) A high-resolution dialysis

712   technique for rapid determination of dissolved reactive phosphate and ferrous iron in pore

713   water of sediments. Science of the Total Environment 421, 245-252.

714   Yu, T., Zhang, Y., Wu, F.C. and Meng, W. (2013) Six-Decade Change in Water Chemistry of

715   Large Freshwater Lake Taihu, China. Environmental Science & Technology 47(16), 9093-

716   9101.

717   Zak, D., Kleeberg, A. and Hupfer, M. (2006) Sulphate-mediated phosphorus mobilization in

718   riverine sediments at increasing sulphate concentration, River Spree, NE Germany.

719   Biogeochemistry 80(2), 109-119.

720   Zhao, Y.P., Zhang, Z.Q., Wang, G.X., Li, X.J., Ma, J., Chen, S., Deng, H. and Annalisa, O.H.

721   (2019) High sulfide production induced by algae decomposition and its potential

722   stimulation to phosphorus mobility in sediment. Science of the Total Environment 650, 163-

723   172.

724   Zilius, M., De Wit, R. and Bartoli, M. (2016) Response of sedimentary processes to

725   cyanobacteria loading. Journal of limnology 75(2), 236-247.

726

727